selected for simulating diffraction fields since the geometry of the plate and the ECCD array is symmetrical.

We investigate the possibility to reduce sidelobes of the ECCD array by mounting a finite reflected plate below the array. It is well known that dipoles with infinite ground plane can achieve the maximum gain if the height of dipoles over the ground is 0.25 wavelength. Extensive calculations in this paper have indicated that a finite reflected plate with an appropriate size can also achieve the same effects for increasing gain and reducing sidelobes as an infinite plate. It has been observed from Fig. 5 that the height of 0.25 wavelengths actually achieves a greatly reduced sidelobes as well as the maximum gain. This is because the diffraction by finite edges of the plate is quite small, compared to reflection from the surface of plate. The total scattering field over the above half-space of a finite plate is almost equal to the sum of two parts, one is from the direct radiation of antennas and the other from full reflection due to the ground plate. The above results are just desired for some radars to increase gain and to block ground clutter signals.

Based on the above simulations, we adopt a 22 by 24 planar ECCD array to the LTR shown in Fig. 6. The LTR is a 1.36-GHz pulse-modulated monostatic Doppler radar with an active phased array system, where the antennas consists of two rectangular arrays, they are perpendicularly superimposed corresponding to two linear polarization. The configuration of each array is the same as that mentioned in Section III. The nominal peak power is 2 kW (the maximum average power is 400 W), which is produced by 24 solid state power amplifiers (transmitter modules). The LTR has been successfully operated at the Shigaraki MU radar observatory of Kyoto University for the lower atmosphere observation.

V. Conclusion

An efficient analysis procedure is presented for exactly modeling the far field of ECCD element. One of its advantages is that one need not handle infinite integrals raised [1] for the process is based on Pocklington type of formulation that only involves closed form of Green's functions in free space. This allows the proposed analysis process in this paper to be easily applied to various ECCD elements with different lengths and radii of circular pipe. Owing to its advantages of simply constructed and clear physical meanings, the procedure in this paper, compared to available methods from other literatures, can also be more easily applied in engineering.

The equivalent model derived from the analysis for the ECCD element can result in the simplification for the computation of the radiation pattern of the ECCD under some special conditions, and therefore can increase computation efficiency.

It is fully novel configuration in the ECCD application to mount a large ECCD planar array over a finite metallic reflected plate with a suitable height so as to achieve reduced radiation sidelobes of array antenna. The uniform physical theory of diffraction, being hybrid with the proposed method for the ECCD element, has handled successfully the scattered far field of this system, the proposed height for ECCD array antenna over the plate is practical useful.

The proposed ECCD array configuration in the LTR is only a start for ECCD array application. Authors believe that the related configuration can also be expected to application in other fields, such as based station antennas for wireless communications.

Acknowledgment

This work has benefited from the input of Mitsubishi Electric Corporation (MELCO), Kanagawa, Japan. The authors are grateful for useful discussions with Dr. Miyashita of MELCO.

References

[1] H. Miyashita, H. Ohmine, K. Nishizawa, S. Makino, and S. Urasaki, "Electromagnetically coupled coaxial dipole array antenna," *IEEE Trans. Antennas Propagat.*, vol. 47, no. 11, pp. 1716–1725, Nov. 1999.

[2] H. Miyashita, "Study on analytical modeling of anatenna arrays for implementation of efficient design procedure," Ph.D. dissertation, Radio Science Center for Space and Atmosphere, Kyoto University, ch. 2, May 2000.

[3] L. L. Tsai, "A numerical solution for the near and far fields of an annular ring of magnetic current," *IEEE Trans. Antennas Propagat.*, vol. AP-20, pp. 569–576, Sept. 1972.

[4] E. Yamashita, *Analysis Methods for Electromagnetic Wave Problems*. Norwood, MA: Artech House, 1996, Physical Optics by Makoto Ando, ch. 4.

[5] A. K. Bhattacharyya, *High Frequency Electromagnetic Techniques: Recent Advances and Applications*. New York: Wiley, 1995.

Radar Cross Section of Stacked Circular Microstrip Patches on Anisotropic and Chiral Substrates

V. Losada, R. R. Boix, and F. Medina

***Abstract*—Galerkin's method in the Hankel transform domain (HTD) is applied to the determination of the radar cross section (RCS) of stacked circular microstrip patches fabricated on a two-layered substrate which may be made of a uniaxial anisotropic dielectric, a magnetized ferrite or a chiral material. Concerning the case of stacked patches printed on magnetized ferrites, the results show that substantial RCS reduction can be achieved inside the tunable frequency band where magnetostatic mode propagation is allowed. It is also shown that both the frequency and the level of the RCS peaks obtained for circular patches fabricated on anisotropic dielectrics or chiral materials may be substantially different from those obtained when substrate anisotropy or substrate chirality are ignored.**

***Index Terms*—Anisotropic media, chiral media, ferrites, microstrip antennas, scattering.**

I. Introduction

Although the standard configuration for a microstrip antenna involves one single conductor patch, two stacked conductor patches are sometimes employed for obtaining either dual-frequency operation [1] or increased bandwidth operation [1], [2]. Concerning the topic of scattering from microstrip antennas, we should say that as the radar cross section (RCS) of military platforms is reduced by geometrical shaping and the use of composite radar absorbing materials, the scattering from the antennas mounted on such structures may give the most important contribution to the overall RCS. Bearing in mind that microstrip antennas are very suitable for use on aircraft vehicles owing to their light weight and conformability, different results were published in the past for the RCS of single microstrip antennas both on conventional isotropic dielectric substrates [3] and nonconventional substrates with dielectric and magnetic anisotropy [4], [5]. The feeding and radiation

Manuscript received September 28, 2001; revised January 28, 2002. This work was supported by the El Centro de Investigación Científica y Tecnológica (CICYT), Spain under Grant TIC98-0630.

V. Losada is with the Microwaves Group, Department of Applied Physics, E.U.I.T.A., University of Seville, 41013, Sevilla, Spain.

R. R. Boix and F. Medina are with the Microwaves Group, Department of Electronics and Electromagnetism, College of Physics, University of Seville, 41012 Sevilla, Spain (e-mails: boix@us.es; medina@us.es).

Digital Object Identifier 10.1109/TAP.2003.811528

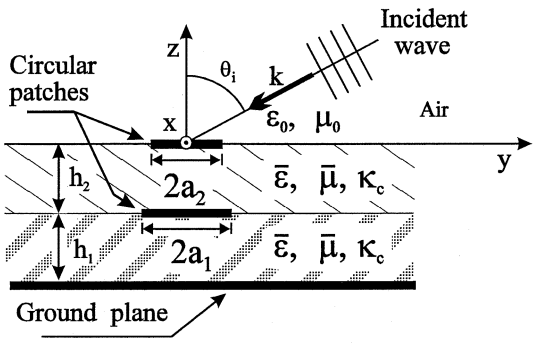

(a)

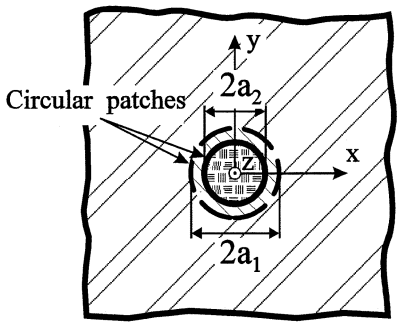

(b)

Fig. 1. Side (a) and top (b) views of two stacked circular microstrip patches fabricated on a two-layered substrate which may be made of a uniaxial anisotropic dielectric, a magnetized ferrite or a chiral material. A plane wave whose direction of propagation makes an angle $\boldsymbol{\theta}_i$ with the $\boldsymbol{z}$ axis incides on the stacked circular patches.

properties of microstrip antennas fabricated on chiral substrates have also been analyzed in detail [6], but the study of the scattering from this type of antennas is a topic which has not received much attention. In this paper the authors apply Galerkin's method in the Hankel transform domain (HTD) [7], [8] to the determination of the RCS of unloaded stacked circular microstrip patch antennas fabricated on a two-layered substrate which may be made of a uniaxial anisotropic dielectric, a magnetized ferrite or a chiral material. Although the topic of the scattering from isolated microstrip patches has been extensively treated [3]–[5], to the authors' knowledge, this is the first paper dealing with the determination of the RCS of stacked microstrip patches fabricated on complex materials.

II. Problem Geometry

Fig. 1 shows the side and top views of two stacked circular microstrip patches of radii a_1 and a_2 placed above a ground plane. The revolution axis of the two circular patches is assumed to be the z axis of Fig. 1. The circular metallic patches and the ground plane are assumed to be perfect electric conductors (PEC) of negligible thickness. The substrate is assumed to be made of two layers of the same material which infinitely extend along the x and y coordinates. The material of the two-layered substrate is chosen among three different possibilities: a uniaxial anisotropic dielectric, a normally biased ferrite and a chiral material. In case the substrate is a uniaxial anisotropic dielectric [4], it will be assumed that its permeability is μ_0 and its permittivity tensor is of the form shown in [8, eq. (1)] (i.e, the elements of the permittivity tensor can be obtained in terms of transverse and axial relative permittivities ϵ_t and ϵ_z). In case the substrate is a magnetized ferrite, it will be assumed that the ferrite is magnetically saturated, and that the bias magnetic field of the ferrite is directed along the z axis of Fig. 1. For that particular case, the permittivity of the ferrite material will be taken as $\epsilon_0\epsilon_f$ and the permeability tensor will be taken as that shown in [8, eq. (2)] (the elements of the permeability tensor can be obtained in terms of the gyromagnetic ratio $\gamma = 1.759 \cdot 10^{11}$ C/Kg, the saturation magnetization of the ferrite material M_s, the internal bias magnetic field H_0 and the linewidth ΔH as explained in [9]). Finally, if the substrate of Fig. 1 is a chiral material, this material will be assumed to be a Pasteur medium [10] with permittivity $\epsilon_0\epsilon_c$, permeability $\mu_0\mu_c$ and dimensionless chiral parameter κ_c. Inside this chiral material, the constitutive relations among the four vector quantities $\mathbf{D}$, $\mathbf{B}$, $\mathbf{E}$, and $\mathbf{H}$ will be those shown in [8, eqs. (3) and (4)].

III. Solution Method

Let us assume that a TEM plane wave travelling through the air incides on the stacked patches of Fig. 1. The incident wave will be both reflected by the two-layered substrate and scattered by the two metallic circular patches. If the total tangential electric field on every patch (sum of the tangential electric fields of the incident wave, the reflected wave and the scattered wave) is obliged to be zero, a set of two electric field integral equations (EFIEs) for the induced current densities on the patches is obtained. In order to solve these two EFIEs, in the current paper the authors have expressed the unknown current densities on the patches in cylindrical coordinates, $\mathbf{j}_i = \mathbf{j}_i(\rho,\phi)(i = 1,2)$, as Fourier series of the cylindrical coordinate ϕ given by

$$\mathbf{j}_i(\rho,\phi) = \sum_{m=-\infty}^{+\infty} \mathbf{j}_i^m(\rho) e^{jm\phi} = \sum_{m=-\infty}^{+\infty} \left(j_{i,\rho}^m(\rho)\hat{\boldsymbol{\rho}} + j_{i,\phi}^m(\rho)\hat{\boldsymbol{\phi}} \right) e^{jm\phi} \quad (i = 1,2). \tag{1}$$

Bearing in mind (1), the two original EFIEs have been written in the HTD in order to obtain an infinite set of decoupled pairs of equations for the Hankel transforms of $\mathbf{j}_1^m(\rho)$ and $\mathbf{j}_2^m(\rho)(m = \ldots,-1,0,1,\ldots)$. Each decoupled pair of equations has been solved by applying Galerkin's method in the HTD as in [7]. The basis functions for $j_{i,\rho}^m(\rho)$ and $j_{i,\phi}^m(\rho)(i = 1,2; m = \ldots,-1,0,1,\ldots)$ have been chosen to be those shown in [8, eqs. (10)–(13)]. Once the different functions $\mathbf{j}_i^m(\rho)$ of (1) have been calculated, the far zone scattered electric field $\mathbf{E}_{\rm sc}^{\rm ff}(r,\theta,\phi)$ has been computed in terms of the Hankel transforms of $\mathbf{j}_i^m(\rho)$ by applying the stationary phase method (see [7, eqs. (23) and (24)]), and the different components of the monostatic RCS $\sigma_{\rm uv}^{\rm ms}(u,v = \theta,\phi)$ of the circular patch of Fig. 1 (relating the v component of the scattered electric field and the u component of the incident electric field) have been determined in terms of $\mathbf{E}_{\rm sc}^{\rm ff}(r,\theta = \theta_i,\phi = \phi_i)$.

IV. Numerical Results

In order to check the validity of the algorithm described in Section II, in Fig. 2 our numerical results for the RCS of stacked circular patches fabricated on a isotropic dielectric substrate are compared with the results obtained by means of the electromagnetic simulator "ensemble." Good agreement exists between the two sets of results. The resonant frequencies indicated by the arrows of Fig. 2 have been obtained by means of an extension of the method reported in [7]. Note that the resonances appear in pairs in accordance with the fact that the stacked patches represent a system of coupled resonators. The results of Fig. 2 for the RCS of stacked circular patches have not only been compared with the results supplied by "ensemble" but also with those obtained when the lower patch is absent. It can be seen that the results for the isolated upper patch match pretty well those obtained for the stacked patches, except in the neighborhood of the resonances related to the

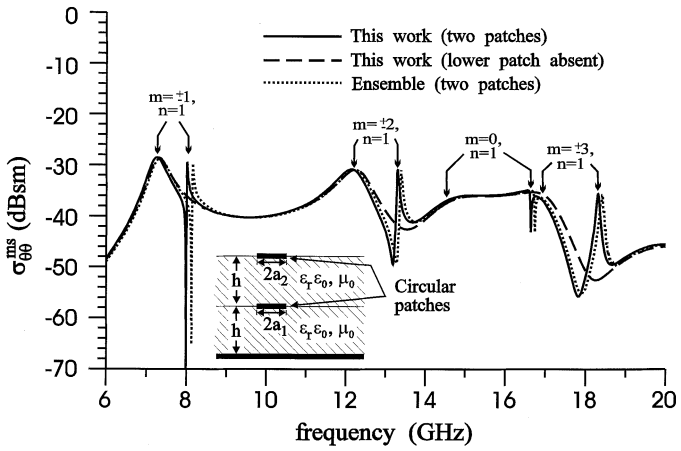

Fig. 2. Monostatic RCS component $\boldsymbol{\sigma}_{\theta\theta}^{\mathrm{ms}}$ of stacked circular microstrip patches versus frequency ($\boldsymbol{\theta}_i = \mathbf{63}^\circ$, $\boldsymbol{a}_1 = \mathbf{7.1}$ mm, $\boldsymbol{a}_2 = \mathbf{7.25}$ mm). The substrate chosen is an isotropic dielectric ($\boldsymbol{h} = \mathbf{0.7874}$ mm, $\boldsymbol{\epsilon}_r = \mathbf{2.2}$). Our results for stacked patches (solid lines) are compared with those obtained by means of ensemble (dotted lines), and with our results for the case where the lower patch is absent (dashed line). The vertical arrows locate the resonant frequencies of the stacked patches.

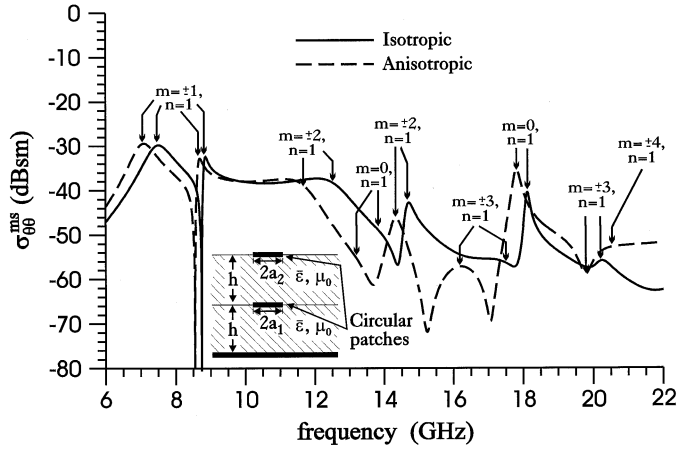

Fig. 3. Monostatic RCS component $\boldsymbol{\sigma}_{\theta\theta}^{\mathrm{ms}}$ of stacked circular microstrip patches versus frequency ($\boldsymbol{\theta}_i = \mathbf{60}^\circ$, $\boldsymbol{a}_1 = \mathbf{5}$ mm, $\boldsymbol{a}_2 = \mathbf{5.1}$ mm). The substrate is taken to be either isotropic P.B.N. ($\boldsymbol{h} = \mathbf{1.27}$ mm, $\boldsymbol{\epsilon}_t = \boldsymbol{\epsilon}_z = \mathbf{3.4}$) or anisotropic P.B.N. ($\boldsymbol{h} = \mathbf{1.27}$ mm, $\boldsymbol{\epsilon}_t = \mathbf{5.12}$, $\boldsymbol{\epsilon}_z = \mathbf{3.4}$).

lower patch. These latter resonances present very large quality factors and can be identified as very large peaks in the RCS curves of the stacked patches.

In Fig. 3 results are plotted for the copolarized RCS component $\sigma_{\theta\theta}^{\mathrm{ms}}$ of stacked circular microstrip patches fabricated on an anisotropic dielectric substrate (pyrolitic boron nitride). The cross-polarized component $\sigma_{\theta\phi}^{\mathrm{ms}}$ is zero as it happens in the isotropic case (see Fig. 2). In Fig. 3 the results obtained for the RCS of patches on an anisotropic substrate are compared with the results that would be obtained if dielectric anisotropy were neglected. It can be checked that the differences between the anisotropic resonant peaks and the isotropic resonant peaks are around 7% in the case of resonances related to the upper patch, and around 2% in the case of resonances related to the lower patch, which indicates that the effect of anisotropy is more pronounced in the former resonances than in the latter resonances. Note that in Fig. 3 the differences between the shapes of the two RCS curves (including the level of the RCS peaks) become more relevant as the frequency increases (especially, beyond 11 GHz), which implies that the effect of anisotropy

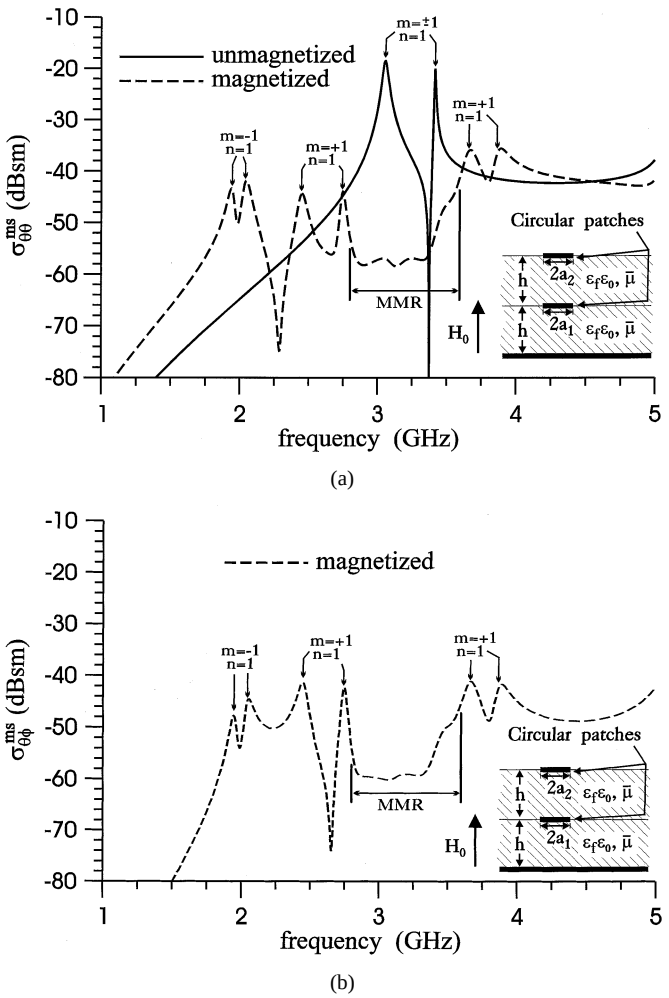

Fig. 4. Monostatic RCS components $\boldsymbol{\sigma}_{\theta\theta}^{\mathrm{ms}}$ (a) and $\boldsymbol{\sigma}_{\theta\phi}^{\mathrm{ms}}$ (b) of stacked circular microstrip patches versus frequency ($\boldsymbol{\theta}_i = \mathbf{60}^\circ$, $\boldsymbol{a}_1 = \mathbf{6.25}$ mm, $\boldsymbol{a}_2 = \mathbf{6.5}$ mm). The substrate is taken to be a ferrite material ($\boldsymbol{h} = \mathbf{1.27}$ mm, $\boldsymbol{\epsilon}_f = \mathbf{15}$) which can be unmagnetized ($\boldsymbol{M}_s = \boldsymbol{H}_0 = \boldsymbol{\Delta H} = 0$) or magnetized ($\boldsymbol{\mu}_0 \boldsymbol{M}_s = \mathbf{0.065}$ T, $\boldsymbol{\mu}_0 \boldsymbol{H}_0 = \mathbf{0.1}$ T, $\boldsymbol{\mu}_0 \boldsymbol{\Delta H} = \mathbf{0.004}$ T). MMR is the acronym for the magnetostatic mode region.

on the RCS values of the stacked patches increases as the frequency increases.

In Fig. 4 (a) and (b) the authors present results for the RCS components $\sigma_{\theta\theta}^{\mathrm{ms}}$ and $\sigma_{\theta\phi}^{\mathrm{ms}}$ of stacked circular microstrip patches fabricated on a ferrite substrate. Note that as the ferrite is magnetized, there is a whole frequency interval 2.8 GHz $< f <$ 3.4 GHz where the two components of the RCS stay below -55 dBsm. This is based on the fact that the stacked microstrip patches fabricated on magnetized ferrite substrate cannot resonate in the frequency band $\mu_0\gamma H_0/2\pi < f < \mu_0\gamma\sqrt{H_0(H_0+M_s)}/2\pi$ (denoted as MMR in the figures) owing to the propagation of an infinite number of magnetostatic volume-wave modes along the conductor-backed ferrite slab supporting the two stacked patches (see Fig. 3 of [8]). Thus, the results of Fig.4 (a) and (b) indicate that microstrip patches fabricated on ferrite substrates present a whole frequency band with very low values of RCS which can be tuned by adjusting the magnitude of the bias magnetic field H_0.

In Fig. 5 (a) and (b) the results obtained for the RCS components $\sigma_{\theta\theta}^{\mathrm{ms}}$ and $\sigma_{\theta\phi}^{\mathrm{ms}}$ of stacked circular microstrip patches fabricated on chiral substrates are compared with the results obtained for the stacked patches when the chiral parameter is set to zero. Fig.5 (a) shows that the differences between the frequencies of the RCS peaks obtained in the chiral

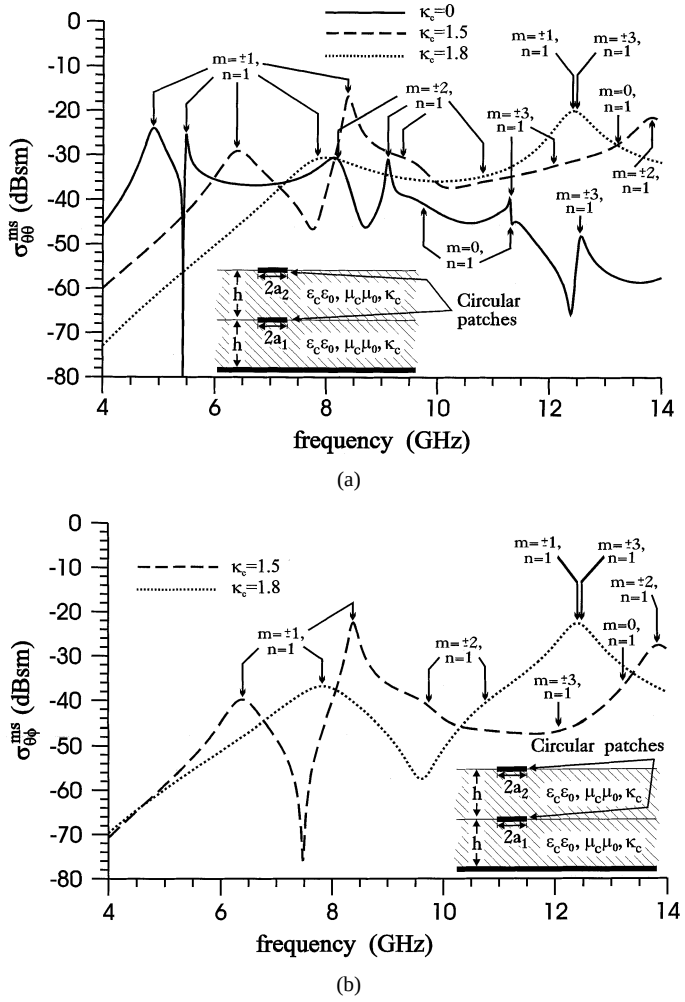

Fig. 5. Monostatic RCS components $\boldsymbol{\sigma}_{\theta\theta}^{\mathrm{ms}}$ (a) and $\boldsymbol{\sigma}_{\theta\phi}^{\mathrm{ms}}$ (b) of stacked circular microstrip patches versus frequency ($\boldsymbol{\theta}_i = \mathbf{60}^\circ$, $\boldsymbol{a}_1 = \mathbf{7.62}$ mm, $\boldsymbol{a}_2 = \mathbf{7.77}$ mm).The substrate is taken to be either a nonchiral dielectric material ($\boldsymbol{h} = \mathbf{1.27}$ mm, $\boldsymbol{\epsilon}_c = 4$, $\boldsymbol{\mu}_c = 1$, $\boldsymbol{\kappa}_c = 0$) or chiral materials with different values of $\boldsymbol{\kappa}_c$ ($\boldsymbol{h} = \mathbf{1.27}$ mm, $\boldsymbol{\epsilon}_c = 4$, $\boldsymbol{\mu}_c = 1$).

case and those obtained in the nonchiral case are more pronounced for the resonances related to the lower patch than for the resonances related to the upper patch (in fact, whereas these differences reach 31% when $\kappa_c = 1.5$ and 63% when $\kappa_c = 1.8$ in the resonances related to the upper patch, the same differences reach 53% when $\kappa_c = 1.5$ and 126% when $\kappa_c = 1.8$ in the resonances related to the lower patch). Also, in Fig. 5 (a) and (b) the RCS peaks related to resonances of the lower patch are in the chiral case around 14 dBsm above those related to resonances of the upper patch. All this indicates that the effect of substrate chirality on the RCS values of stacked microstrip patches is much more pronounced in the resonances related to the lower patch than in those related to the upper patch.

V. Conclusion

Galerkin's method in the HTD has been used for the numerical determination of the RCS of stacked circular microstrip patches fabricated on a two-layered substrate which may be made of a uniaxial anisotropic dielectric, a magnetized ferrite or a chiral material. Concerning the RCS values of patches fabricated on anisotropic dielectrics and chiral media, the results show that whereas substrate dielectric anisotropy has a more pronounced effect on the resonances related to the upper patch than on the resonances related to the lower patch, substrate chirality has just the opposite effect. In the case of stacked patches fabricated on ferrite substrates, the results obtained show that substantial RCS reduction can be achieved in a whole frequency band, and that this frequency band can be adjusted by varying the bias magnetic field of the ferrite substrates.

References

[1] L. Barlatey, J. R. Mosig, and T. Sphicopoulos, "Analysis of stacked microstrip patches with a mixed potential integral equation," *IEEE Trans. Antennas Propagat.*, vol. 38, pp. 608–615, May 1990.

[2] F. Croq and D. M. Pozar, "Millimeter—wave design of wide-band aperture-coupled stacked microstrip antennas," *IEEE Trans. Antennas Propagat.*, vol. 39, pp. 1770–1776, Dec. 1991.

[3] J. T. Aberle, D. M. Pozar, and C. R. Bitcher, "Evaluation of input impedance and radar cross section of probe-fed microstrip patch elements using an accurate feed model," *IEEE Trans. Antennas Propagat.*, vol. 39, pp. 1691–1696, Dec. 1991.

[4] D. M. Pozar, "Radiation and scattering from a microstrip patch on a uniaxial substrate," *IEEE Trans. Antennas Propagat.*, vol. AP-35, pp. 613–621, June 1987.

[5] H. Y. Yang, J. A. Castaneda, and N. G. Alexopoulos, "The RCS of a microstrip patch on an arbitrarily biased ferrite substrate," *IEEE Trans. Antennas Propagat.*, vol. 41, pp. 1610–1614, Dec. 1993.

[6] A. Toscano and L. Vegni, "Analysis of printed-circuit antennas with chiral substrates with the method of lines," *IEEE Trans. Antennas Propagat.*, vol. 49, pp. 48–53, Jan. 2001.

[7] V. Losada, R. R. Boix, and M. Horno, "Resonant modes of circular microstrip patches in multilayered substrates," *IEEE Trans. Microwave Theory Tech.*, vol. MTT-47, pp. 488–498, Apr. 1999.

[8] ——, "Full-wave analysis of circular microstrip resonators in multilayered media containing uniaxial anisotropic dielectrics, magnetized ferrites, and chiral materials," *IEEE Trans. Microwave Theory Tech.*, vol. 48, pp. 1057–1064, June 2000.

[9] D. M. Pozar, *Microwave Engineering*. Reading, MA: Addison-Wesley, 1990.

[10] I. V. Lindell, A. H. Sihvola, S. A. Tretyakov, and A. J. Viitanen, *Electromagnetic Waves in Chiral and Bi-Isotropic Media*. Norwood, MA: Artech House, 1994.